Motion Estimation Model for Cardiac and Respiratory Motion Compensation

Sebastian Kaeppler[1], Alexander Brost[1,⋆], Martin Koch[1], Wen Wu[2], Felix Bourier[3], Terrence Chen[2], Klaus Kurzidim[3], Joachim Hornegger[1], and Norbert Strobel[4]

[1] Pattern Recognition Lab, Friedrich-Alexander-University Erlangen-Nuremberg, Erlangen, Germany
Alexander.Brost@cs.fau.de
[2] Siemens Corporation, Corporate Research and Technology, NJ, USA
[3] Klinik für Herzrhythmusstörungen, Krankenhaus Barmherzige Brüder, Regensburg, Germany
[4] Siemens AG, Healthcare Sector, Forchheim, Germany

Abstract. Catheter ablation is widely accepted as the best remaining option for the treatment of atrial fibrillation if drug therapy fails. Ablation procedures can be guided by 3-D overlay images projected onto live fluoroscopic X-ray images. These overlay images are generated from either MR, CT or C-Arm CT volumes. As the alignment of the overlay is often compromised by cardiac and respiratory motion, motion compensation methods are desirable. The most recent and promising approaches use either a catheter in the coronary sinus vein, or a circumferential mapping catheter placed at the ostium of one of the pulmonary veins. As both methods suffer from different problems, we propose a novel method to achieve motion compensation for fluoroscopy guided cardiac ablation procedures. Our new method localizes the coronary sinus catheter. Based on this information, we estimate the position of the circumferential mapping catheter. As the mapping catheter is placed at the site of ablation, it provides a good surrogate for respiratory and cardiac motion. To correlate the motion of both catheters, our method includes a training phase in which both catheters are tracked together. The training information is then used to estimate the cardiac and respiratory motion of the left atrium by observing the coronary sinus catheter only. The approach yields an average 2-D estimation error of 1.99 ± 1.20 mm.

1 Introduction

An irregular fast rhythm of the left atrium - clinically described as atrial fibrillation - may cause blood clotting which bears a high risk of stroke [1]. If drug therapy is not an option, catheter ablation is the standard treatment option [2]. Catheter ablation procedures are guided by fluoroscopic images obtained from C-arm systems. Important targets of the ablation procedure are the ostia of the pulmonary veins. The goal of the ablation procedure is to create a continuous

⋆ Corresponding author.

P. Abolmaesumi et al. (Eds.): IPCAI 2012, LNAI 7330, pp. 94–103, 2012.

lesion set around these pulmonary veins to electrically isolate them from the left atrium. In general three catheters are used during the procedure. At the beginning of the procedure, a linear catheter is placed inside the coronary sinus vein, where it is to remain fixed during the procedure. It is referred to as CS catheter. The coronary sinus vein lies between the left ventricle and the left atrium. Then, an ablation catheter and a circumferential mapping catheter are brought into the left atrium by means of two transseptal punctures. For pulmonary vein isolation, the mapping catheter is positioned at the ostium of each of the pulmonary veins (PVs) considered for ablation, in order to measure electrical signals. As the soft-tissue ablation targets inside the heart are not visible within X-ray images [3,4], overlay images generated from either CT, MR, or C-arm CT can be used during the procedures to facilitate a more accurate catheter navigation [5]. Unfortunately, the clinical value of these overlay images is reduced by cardiac and respiratory motion.

Recent approaches for motion compensation based on tracking of the CS or the circumferential mapping catheter have shown to improve the alignment of these overlay images [6,7]. The work in [6] facilitates motion compensation by using the CS catheter, whereas the method in [7] uses the circumferential mapping catheter. The downside of using the CS catheter to derive a motion estimate for animating the overlay image is due to the fact that this catheter is outside of the left atrium and close to the left ventricle. Therefore, its movement is strongly influenced by ventricular motion. This is why other authors [8] found it to be unsuitable for cardiac motion compensation in ablation procedures. The circumferential mapping catheter on the other hand has the advantage that it can be placed close to the site of ablation. In this case, the calculated catheter position can be used directly to update the overlay images. Unfortunately, relying on the mapping catheter is not without problems. For example, it may be moved on purpose during the procedure, e.g., to reposition it from one PV to another. Detecting when to stop motion compensation then either requires user interaction or a movement detection algorithm. In addition, if only one transseptal puncture is performed, only one catheter can be inside the left atrium. In this case, the circumferential mapping catheter is brought into the left atrium before and after the ablation of one PV to measure the electrical signals. Thus it may not even be avilable for motion compensation during the ablation itself. This is why we propose a new method that combines the advantage of the coronary sinus catheter, its continuous presence throughout the procedure, with the accuracy of the mapping catheter. To this end, we use a training phase during which both catheters are tracked. The acquired data is then used to set up an estimation model for the position of the mapping catheter. After that, the model can be used to estimate the cardiac and respiratory motion of the left atrium by observing the CS catheter only.

2 Motion Compensation

In order to improve the motion compensation results, we separate the motion of the CS catheter into respiratory and cardiac motion. For respiratory motion, a rigid approximation of the heart motion has shown to give good results [9]. Here, we assume that both the CS and the mapping catheter are equally affected by respiratory movement. The heart beat related motion patterns of the two catheters, however, usually differ. The displacement between the two catheters due to different cardiac motion patterns may exceed 10 mm, see Fig. 3. We use the position of the CS catheter to determine the cardiac phase of an image. Using the training data, we estimate the position of the circumferential mapping catheter based on the cardiac phase. This way we compensate for the difference in cardiac motion between the two catheters. Our method is separated into three steps. The first step is the training phase in which both the CS and the mapping catheter are tracked together. In the second step, we compute features to relate the CS catheter position to a point in the cardiac cycle. The third step is the actual live motion compensation during the procedures. The details are given in the following subsections.

2.1 Training Phase

For every image in the training phase, the circumferential mapping catheter and the CS catheter are tracked using the method proposed in [10]. The positions of the electrodes of the CS and the center of the mapping catheter are stored for later computations. The tracked electrodes of the CS catheter are denoted as $\boldsymbol{c}_i^{(j)} = (u_i^{(j)}, v_i^{(j)})^T$ with $i \in \{1, 2, ..., N\}$ and N being the number of electrodes, and $j \in [1, M]$ the number of images in the training sequence. Usually, CS catheters with either four or ten electrodes are used during ablation procedures. The center of the mapping catheter in frame j is denoted as $\boldsymbol{m}_j \in \mathbb{R}^2$. The image coordinate system is defined by the coordinates u and v. For simplicity, we denote the most distal electrode as $\boldsymbol{c}_1$ and the most proximal one as $\boldsymbol{c}_N$.

2.2 Motion Estimation Model

In order to build our model, we need to determine the cardiac phase for each training image. One could use ECG data to determine the cardiac phase for a given frame. Unfortunately, this data is not always readily available at the imaging system. Additionally, its accuracy may be affected by irregularities of the heart beat. Here, the computation of the cardiac phase is based on a pattern recognition approach instead. In particular, we exploit the fact that respiration causes only a slight rotational movement of the heart [9,11], while the electrodes of the CS catheter show a large relative rotative movement during the cardiac cycle. We try to capture this movement due to the cardiac cycle using a feature set based on the positions of the electrodes of the CS catheter. For an illustration, see Fig. 1. The following features $f_1^{(j)}, \ldots, f_5^{(j)}$ for image j are computed for all images j in the training set:

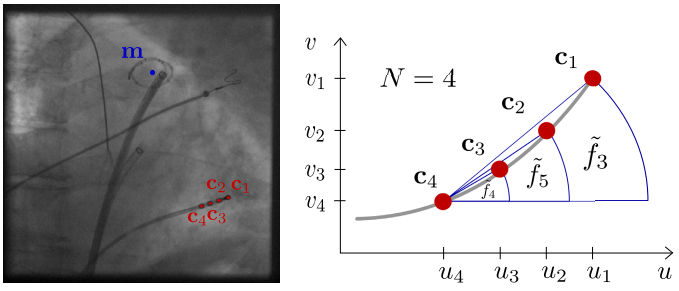

(a) (b)

Fig. 1. Features used to calculate the cardiac cycle value μ. (a) One frame of a typical fluoroscopic sequence. (b) Illustration of the considered features.

– The first feature is the u-position of the most distal electrode divided by the u-position of the most proximal electrode. The positions are in absolute image coordinates and not related to a reference frame

$$f_1^{(j)} = u_1^{(j)} / u_N^{(j)}. \tag{1}$$

– The second feature is calculated similar to the first feature, using the v-coordinates

$$f_2^{(j)} = v_1^{(j)} / v_N^{(j)}. \tag{2}$$

– The third feature is the angle between the u-axis of the image and the line spanned by the most proximal and most distal electrode

$$f_3^{(j)} = \arctan\left(\frac{|v_1^{(j)} - v_N^{(j)}|}{|u_1^{(j)} - u_N^{(j)}|}\right). \tag{3}$$

– The fourth feature is the angle between the u-axis of the image and the line spanned by the most proximal electrode and the one next to it

$$f_4^{(j)} = \arctan\left(\frac{|v_{N-1}^{(j)} - v_N^{(j)}|}{|u_{N-1}^{(j)} - u_N^{(j)}|}\right). \tag{4}$$

– The last feature is the angle between the u-axis of the image and the line spanned by the most proximal electrode and the second next to it

$$f_5^{(j)} = \arctan\left(\frac{|v_{N-2}^{(j)} - v_N^{(j)}|}{|u_{N-2}^{(j)} - u_N^{(j)}|}\right). \tag{5}$$

These features capture CS catheter rotations and deformations, which are typical for cardiac motion. Yet, they are relatively invariant to translation motion, which is characteristically for respiratory motion. As the feature values have different

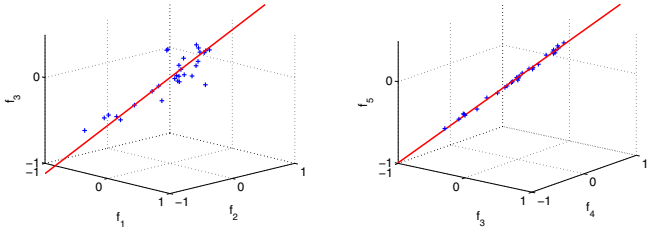

(a) (b)

Fig. 2. Visualization of the feature space. (a) The first three features computed on the training set of sequence #12 (blue cross), and the corresponding principle axis (red line). (b) The last three features computed on the same training set, and the corresponding principle axis.

ranges, they are normalized to the range $[0, 1]$. The resulting features are denoted in vector notation as

$$\boldsymbol{f}_j = (\tilde{f}_1^{(j)}, \tilde{f}_2^{(j)}, \tilde{f}_3^{(j)}, \tilde{f}_4^{(j)}, \tilde{f}_5^{(j)})^T. \tag{6}$$

To reduce the dimensionality of the feature vector, a principle component analysis is performed. First, the mean feature vector is calculated by

$$\bar{\boldsymbol{f}} = \frac{1}{M} \sum_{j=1}^{M} \boldsymbol{f}_j. \tag{7}$$

In the next step, the covariance matrix is calculated by

$$\boldsymbol{\Sigma} = \frac{1}{M-1} \sum_{j=1}^{M} (\boldsymbol{f}_j - \bar{\boldsymbol{f}}) \cdot (\boldsymbol{f}_j - \bar{\boldsymbol{f}})^T. \tag{8}$$

Now, the eigenvalues and eigenvectors of $\boldsymbol{\Sigma}$ are computed. Let $\boldsymbol{e}_\lambda$ be the eigenvector corresponding to the largest eigenvalue of the covariance matrix $\boldsymbol{\Sigma}$. The unitless cardiac cycle value μ_j for every image in the training sequence is finally computed by

$$\mu_j = \boldsymbol{e}_\lambda^T \cdot (\boldsymbol{f}_j - \bar{\boldsymbol{f}}), \tag{9}$$

which is the length of the orthogonal projection of the feature vector onto the first eigenvector. Fig. 2 shows the fit of $\boldsymbol{e}_\lambda$ to the features in feature space. Thus, a correspondence between the calculated cardiac cycle value μ_j and the stored position of the mapping catheter $\boldsymbol{m}_j$ has been established: $\mu_j \rightarrow \boldsymbol{m}_j$. One example of the relationship between μ and the intracardiac motion is depicted in Fig. 3.

2.3 Motion Compensation

For motion compensation, only the tracking results for the CS catheter are required. To apply the compensation, the feature vector needs to be computed

for the new image. This feature vector $\boldsymbol{f}_{\text{new}}$ is calculated from the tracked CS catheter position as described above. The new cycle value is calculated by

$$\mu_{\text{new}} = \boldsymbol{e}_{\lambda}^{T} \cdot (\boldsymbol{f}_{\text{new}} - \bar{\boldsymbol{f}}). \tag{10}$$

In the next step of the motion compensation, two training samples that are closest to the current image with respect to cardiac phase need to be found. The first one, denoted β, is earlier in the cardiac cycle than the new image. The other one, denoted γ, is later. To do so, the following minimization problem is considered for the sample index β:

$$\beta = \underset{\substack{j \\ \mu_j < \mu_{\text{new}}}}{\arg\min} (1 + |\mu_j - \mu_{\text{new}}|)^2 + \alpha \cdot (u_N^{(\text{j})} - u_N^{(\text{new})})^2. \tag{11}$$

For the sample γ, the constraint $\mu_j < \mu_{new}$ in Eq. (11) is replaced by $\mu_j \geq \mu_{new}$. The position of the most proximal electrode in u-direction, $u_N^{(\text{new})}$, is used for regularization. The idea behind this term is to reduce the effect of errors in the calculation of the heart cycle, which may, for example, arrise from slight inaccuracies in the catheter tracking. The cardiac cycle values μ_β and μ_γ correspond to the two samples closest to the new frame with the observed cardiac cycle value μ_{new}. Using these two values, two estimates for the position of the circumferential mapping catheter are computed as

$$\hat{\boldsymbol{m}}_{\text{new},\beta} = \boldsymbol{m}_\beta + \left(\boldsymbol{c}_N^{(\text{new})} - \boldsymbol{c}_N^{(\beta)} \right), \tag{12}$$

$$\hat{\boldsymbol{m}}_{\text{new},\gamma} = \boldsymbol{m}_\gamma + \left(\boldsymbol{c}_N^{(\text{new})} - \boldsymbol{c}_N^{(\gamma)} \right). \tag{13}$$

The difference terms in Eqs. (12, 13) provide the compensation for respiratory motion. For two images in the same cardiac phase, we assume that any remaining motion must be due to respiration. Since we also assume that the CS and the mapping catheter are equally affected by respiratory motion, we simply apply the difference vector between the proximal electrodes of the CS catheter in the two images to the estimate of the position of the mapping catheter. The proximal electrode was chosen because it shows the least intracardiac motion w.r.t. the mapping catheter. These two values are combined to calculate the final estimate as

$$\hat{\boldsymbol{m}}_{\text{new}} = \phi \cdot \hat{\boldsymbol{m}}_{\text{new},\beta} + (1 - \phi) \cdot \hat{\boldsymbol{m}}_{\text{new},\gamma}. \tag{14}$$

The scaling value ϕ between the two estimates is calculated by

$$\phi = \frac{|\mu_\gamma - \mu_{\text{new}}|}{|\mu_\gamma - \mu_\beta|}. \tag{15}$$

In case of high acquisition frame rates $\geq$ 15 frames-per-second, we apply a temporal lowpass filter

$$\hat{\boldsymbol{m}}'_{\text{new}} = \delta \cdot \hat{\boldsymbol{m}}_{\text{new}} + (1 - \delta) \cdot \hat{\boldsymbol{m}}_{\text{new}-1}. \tag{16}$$

This is motivated by the fact that the motion of the heart is smooth in high frame rate image sequences.

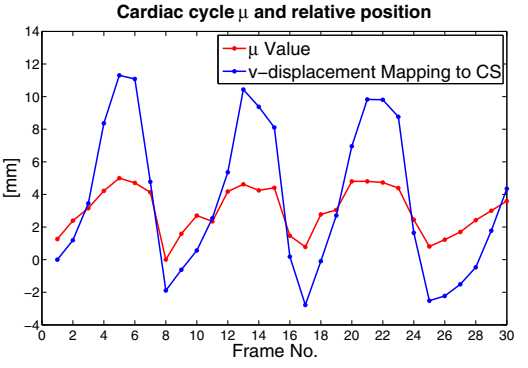

Fig. 3. Calculated μ values for a training set and the displacement between the proximal electrode of the CS and the center of the mapping catheter in v-direction [mm], w.r.t. a reference frame

3 Evaluation and Results

For evaluation, 13 fluoroscopy sequences from three different hospitals were used[1]. The length of the sequences varied between 47 and 150 frames, or two to 47 seconds. Each sequence was split into two disjoint sets of frames. One set, comprising the first 30 frames of the sequence, was used for the patient-specific training of the model. The remaining set was used for evaluation. This resulted in a total number of 958 frames available for evaluation. In a clinical scenario, usually more time passes between training and compensation phase. An evaluation with a simulated clinical workflow is subject of further research. The first sequence was acquired using ECG-triggered fluoroscopy. We chose to include this sequence to see how our method handles respiratory motion with only residual cardiac motion. The other sequences were acquired with either 15 or 30 frames-per-second. We compare our results to an uncompensated overlay as well as to the reference method proposed in [6]. The error is defined as the 2-D Euclidean distance between the estimated position of the overlay, determined by the motion compensation algorithm, and the center of the mapping catheter. Due to its proximity to the ablation target, the motion of the mapping catheter is considered to be the motion that needs to be estimated. For an illustration, see Fig. 5. The values of 0.01 for regularization parameter α and 0.7 for the smoothing parameter δ were determined by performing a grid search on a subsample of the available sequences. The results for the individual sequences are given in Fig. 4. On our available data set, the observed motion was 3.59 mm $\pm$ 2.27 mm. The reference method, proposed in [6,12], yielded an error of 4.65 mm $\pm$ 3.33 mm, which, surprisingly, is higher than the observed motion. Our new approach incorporating the estimation model yielded a compensation error of 1.98 mm $\pm$ 1.30 mm.

[1] The data are available from the authors upon request for non-commercial research.

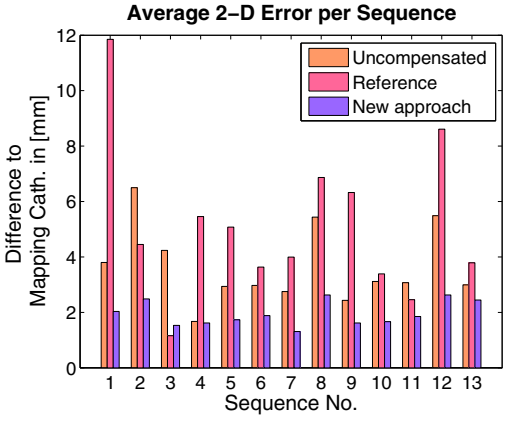

Fig. 4. The results for our motion compensation approach, compared to the reference method in [6], and the misalignment error for an uncompensated approach

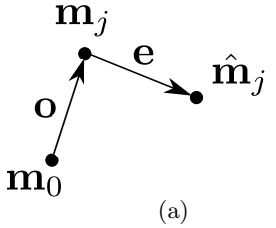

(a)

Frames	Avg. Error [mm]
Uncomp.	3.65 ± 2.36
10	2.87 ± 2.06
20	2.61 ± 1.86
30	2.10 ± 1.35
40	2.01 ± 1.37
50	1.93 ± 1.32

(b)

Fig. 5. Error definition and varying number of training frames. (a) The observed motion $\boldsymbol{o}$ and the estimation error $\boldsymbol{e}$ in frame j. (b) Average error with varying number of training frames. A subset of the complete evauluation set, comprising 701 frames was used to calculate the average error.

4 Discussion and Conclusions

For our datasets, the proposed method has outperformed the reference motion compensation approach proposed in [6,12]. We believe that this is due to the fact that our data was acquired with different X-ray acquisition settings, either regarding frame rate, C-arm position, or both. We also point out that we measured the error on the X-ray detector, whereas in [6,12], it was measured at the iso-center of the C-arm coordinate system. Due to the magnification involved in perspective projection, our error appears larger. Unfortunately, the data used in [6,12] was not available for comparison. The reference method uses a Butterworth low-pass filter to smooth the cardiac motion of the CS catheter and directly applies this motion to the overlay. This approach relies on the assumption that both the CS and the left atrium move in sync, with the CS catheter experiencing a higher amount of cardiac motion compared to the mapping catheter.

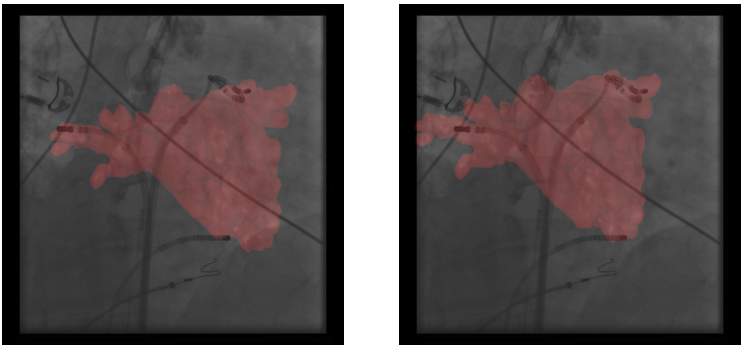

(a) (b)

Fig. 6. A comparison showing the difference if motion compensation is considered or not. (a) One frame without motion compensation. (b) Shows the same frame as in (a), but this time with motion compensation. Best viewed in color.

Another assumption required is that their respective motion directions are the same. The application of a suitably designed lowpass filter can then reduce the amplitude of the cardiac motion estimated from the CS catheter to the amplitude of the cardiac motion of the mapping catheter. Unfortunately, on our data set, these assumptions are not always valid, explaining the higher errors of the reference method. Other researchers also found that the CS and the left atrium need not always follow the same motion pattern [8]. Our estimation model does not depend on these assumptions. In addition, our method does not require older frames for low-pass filtering, making it suitable for low acquisition frame rates. Experiments have shown that about thirty frames are sufficient for the training of our model, see Fig. 5. As expected, both approaches perform not as well as the approach involving the direct tracking of the circumferential mapping catheter [13]. Since the error of our method is still higher than when using the mapping catheter directly, a combination of both methods should be considered. Recent work in [7] already utilized the CS catheter to detect non-physiological movement of the circumferential mapping catheter. In such a case, we may want to switch to CS catheter based motion estimation. Since the currently proposed method deals only with 2-D images, it is prone to suffer from foreshortening which can be difficult to detect in monoplane images. Fortunately, out of plane motion primarily affects the size of the 3-D overlay, and size changes of the left atrium are much less relevant than discrepancies due to heart and breathing motion. The proposed method could be extended to 3-D compensation by performing the training in biplane mode. This way one could estimate 3-D motion while observing 2-D motion. The current implementation of our motion compensation approach achieves about 20 fps. Most of the time per frame is required for catheter tracking. The motion estimation model is calculated within 50 ms. The estimation of the mapping catheter position using the proposed model is performed in less than 10 ms. An example of our motion compensation approach is shown in Fig. 6.

References

1. Wolf, P., Abbott, R., Kannel, W.: Atrial fibrillation as an independent risk factor for stroke: the framingham study. Stroke 22, 983–988 (1991)
2. Cappato, R., Calkins, H., Chen, S.A., Davies, W., Iesaka, Y., Kalman, J., Kim, Y.H., Klein, G., Packer, D., Skanes, A.: Worldwide survey on the methods, efficacy, and safety of catheter ablation for human atrial fibrillation. Circulation 111, 1100–1105 (2005)
3. Prümmer, M., Hornegger, J., Lauritsch, G., Wigström, L., Girard-Hughes, E., Fahrig, R.: Cardiac C-arm CT: a unified framework for motion estimation and dynamic CT. IEEE Transact. Med. Imaging 28(11), 1836–1849 (2009)
4. Strobel, N., Meissner, O., Boese, J., Brunner, T., Heigl, B., Hoheisel, M., Lauritsch, G., Nagel, M., Pfister, M., Rührnschopf, E.-P., Scholz, B., Schreiber, B., Spahn, M., Zellerhoff, M., Klingenbeck-Regn, K.: Imaging with Flat-Detector C-Arm Systems. In: Reiser, M.F., Becker, C.R., Nikolaou, K., Glazer, G. (eds.) Multislice CT (Medical Radiology / Diagnostic Imaging), 3rd edn., pp. 33–51. Springer, Heidelberg (2009)
5. De Buck, S., Maes, F., Ector, J., Bogaert, J., Dymarkowski, S., Heidbüchel, H., Suetens, P.: An Augmented Reality System for Patient-Specific Guidance of Cardiac Catheter Ablation Procedures. IEEE Transact. Med. Imaging 24(11), 1512–1524 (2005)
6. Ma, Y., King, A.P., Gogin, N., Rinaldi, C.A., Gill, J., Razavi, R., Rhode, K.S.: Real-Time Respiratory Motion Correction for Cardiac Electrophysiology Procedures Using Image-Based Coronary Sinus Catheter Tracking. In: Jiang, T., Navab, N., Pluim, J.P.W., Viergever, M.A. (eds.) MICCAI 2010. LNCS, vol. 6361, pp. 391–399. Springer, Heidelberg (2010)
7. Brost, A., Wu, W., Koch, M., Wimmer, A., Chen, T., Liao, R., Hornegger, J., Strobel, N.: Combined Cardiac and Respiratory Motion Compensation for Atrial Fibrillation Ablation Procedures. In: Fichtinger, G., Martel, A., Peters, T. (eds.) MICCAI 2011, Part I. LNCS, vol. 6891, pp. 540–547. Springer, Heidelberg (2011)
8. Klemm, H., Steven, D., Johnsen, C., Ventura, R., Rostock, T., Lutomsky, B., Risius, T., Meinertz, T., Willems, S.: Catheter motion during atrial ablation due to the beating heart and respiration: impact on accuracy and spatial referencing in three-dimensional mapping. Heart Rhythm 4(5), 587–592 (2007)
9. McLeish, K., Hill, D., Atkinson, D., Blackall, J., Razavi, R.: A study of the motion and deformation of the heart due to respiration. IEEE Transact. Med. Imaging 21(9), 1142–1150 (2002)
10. Wu, W., Chen, T., Barbu, A., Wang, P., Strobel, N., Zhou, S., Comaniciu, D.: Learning-based hypothesis fusion for robust catheter tracking in 2D X-ray fluoroscopy. In: IEEE Conference on Computer Vision and Pattern Recognition (CVPR 2011), pp. 1097–1104 (2011)
11. Shechter, G., Ozturk, C., Resar, J., McVeigh, E.: Respiratory motion of the heart from free breathing coronary angiograms. IEEE Transact. Med. Imaging 23(8), 1046–1056 (2004)
12. Ma, Y., King, A., Gogin, N., Gijsbers, G., Rinaldi, C., Gill, J., Razavi, R., Rhode, K.: Clinical evaluation of respiratory motion compensation for anatomical roadmap guided cardiac electrophysiology procedures. IEEE Transact. Biomed. Engineering (2011); Epub ahead of print
13. Brost, A., Liao, R., Hornegger, J., Strobel, N.: Model-based registration for motion compensation during EP ablation procedures. In: Fischer, B., Dawant, B., Lorenz, C. (eds.) WBIR 2010. LNCS, vol. 6204, pp. 234–245. Springer, Heidelberg (2010)